A Multimodal Approach Towards Advancing the Characterization and Analysis of Erbium

Sage Buchanan[1,2], Dr. Lyudmila Goncharova[2,3], Dr. Mark Biesinger[1,3]
[1]Surface Science Western, The University of Western Ontario, London N6G 0J3, ON, Canada
[2]Department of Physics and Astronomy, The University of Western Ontario, London N6G 2V4, ON, Canada
[3]Department of Chemistry, The University of Western Ontario, London N6A 3K7, ON, Canada

Goal: *To enhance the detection, chemical state identification, and recovery capabilities of erbium and other critical rare earth minerals for improved mineral security and economic stability*

Introduction

Erbium is one of the Rare Earth Elements (REE's), the only class of critical minerals* common to all member nations of the Minerals Security Partnership.[1] REE's are **essential to support our advancing and increasingly sustainability focused economies** with applications in all major energy industries, electric vehicles (EV's), advanced consumer electronics, catalysts, and many other areas.

Production challenges and geopolitical tensions are creating **supply chain risks** for REE's. To maintain responsible resource management and disposal strategies, it is crucial to have a comprehensive understanding of the properties and quality of REE-containing materials.

This work is an effort to advance current methodologies surrounding the analysis and characterization of REE's, with a focus on erbium. We present preliminary Rutherford Backscattering Spectroscopy (RBS) results on creating ion-implanted calibration standards for erbium Secondary Ion Mass Spectrometry (SIMS) analyses, and in-depth X-ray Photoelectron Spectroscopy (XPS) studies of erbium standards and REE-containing minerals of significance.

*Critical Minerals:[1]

- "Have few or no substitutes
- Are strategic and somewhat limited commodities; or
- Are increasingly concentrated in terms of extraction and, even more, in terms of processing location"

They are important, and there are risks with their supply chains

Applications of REE's:

- **Permanent magnets**
  - Generators, motors, EV's, MRI's
- **Electronics**
  - LED's, cell phones, batteries, IR optics, LCD screens, speakers
- **Catalysts**
  - Catalytic converters
- **Energy**
  - Nuclear control rods, solar cells, wind turbines, fossil fuel refining

Rare Earth Element Supply Chains

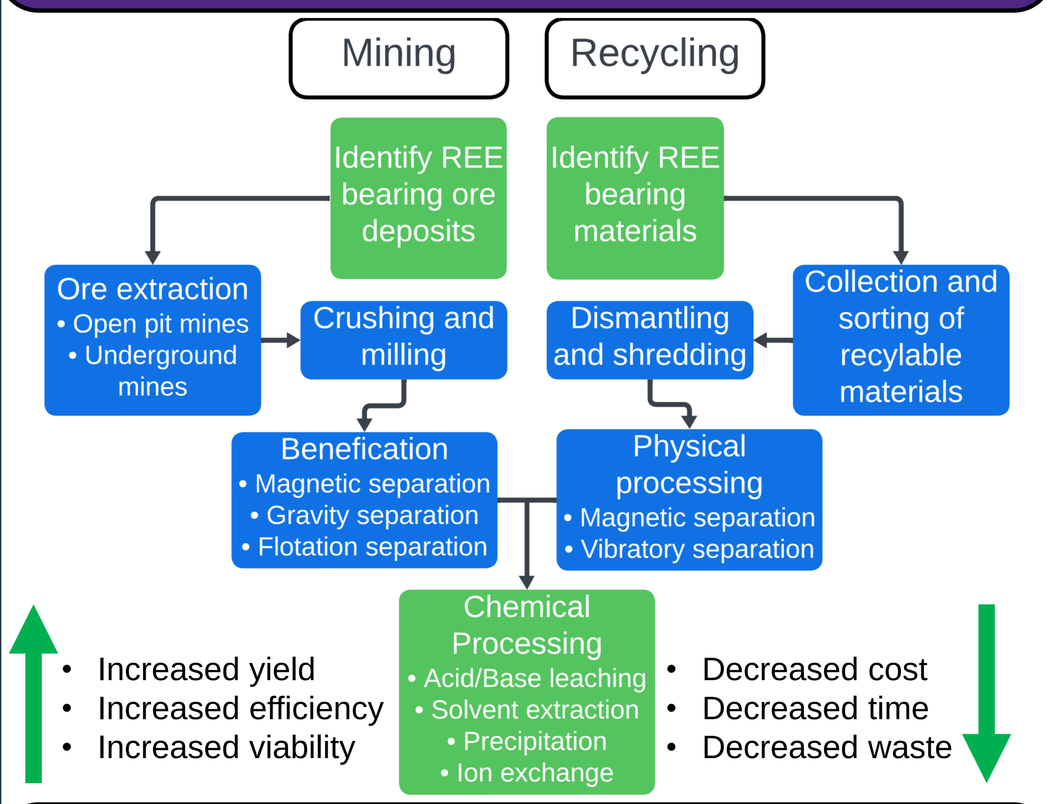

By improving our ability to detect and accurately identify REE's, we support the critical initial and final steps in both streams of the REE supply chain.

Global supply of REE's is still largely monopolized by China, as shown in Figure 1. While a few other countries are (re)emerging as REE producers, **Canada currently produces no REE's commercially** and the U.S. remains >95% reliant on imports for their current REE consumption.[1, 2]

As demand rapidly increases, it is essential to enhance the feasibility and efficiency of REE production through both mining and recycling. Current recovery estimates from mined ores range from 50-80%[4], which we aim to improve upon, alongside strengthened recycling efforts by advancing our abilities to detect and quantify the chemical states of REE's using calibration standards and analyzing reference materials.

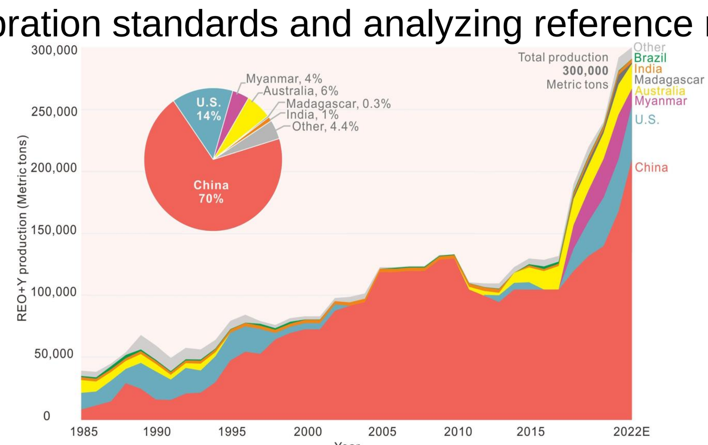

Figure 1: Global mine production by country of yttrium-containing rare earth oxides. Reprinted with permission from Liu et al. [3]

Results – Ion Implantation and RBS

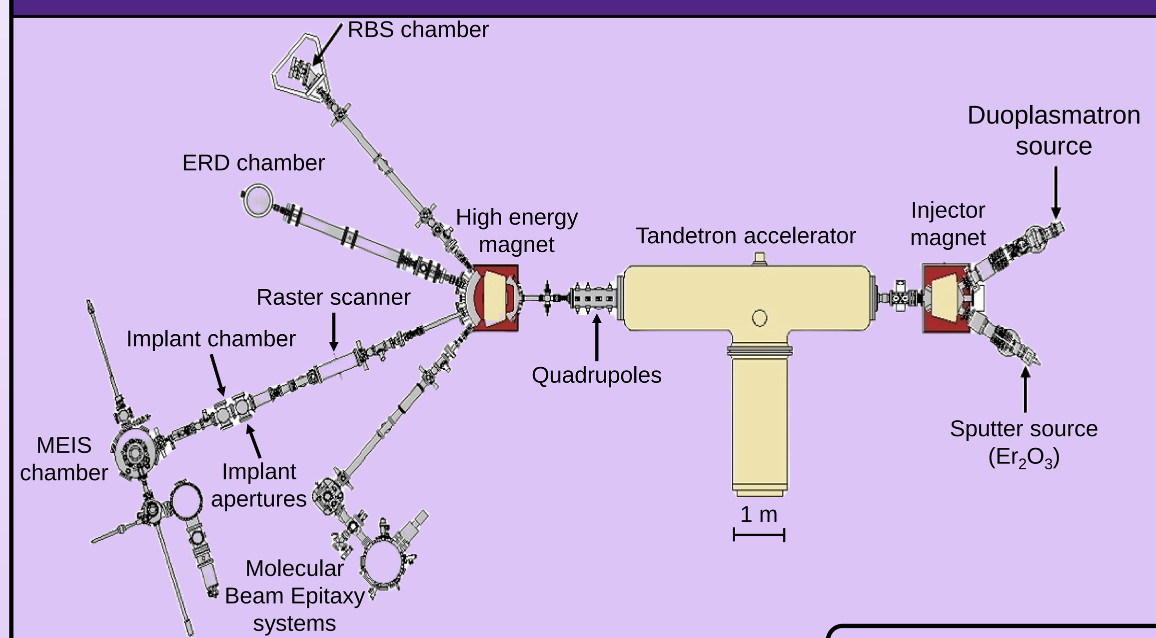

Ion implantation is being tested as a method to create calibration standards for SIMS analyses as known concentrations can be implanted.

Our method involves:

1. Using SRIM[5] simulations to inform implant conditions
2. Implanting Er^+ ions into Si wafers shielded by removable masks via the Tandetron accelerator
   - Masks are used to achieve desired implant depths
3. Conducting RBS with He^+ ions to analyze the depth profiles of the implanted wafers and to evaluate for beam damage and/or contamination

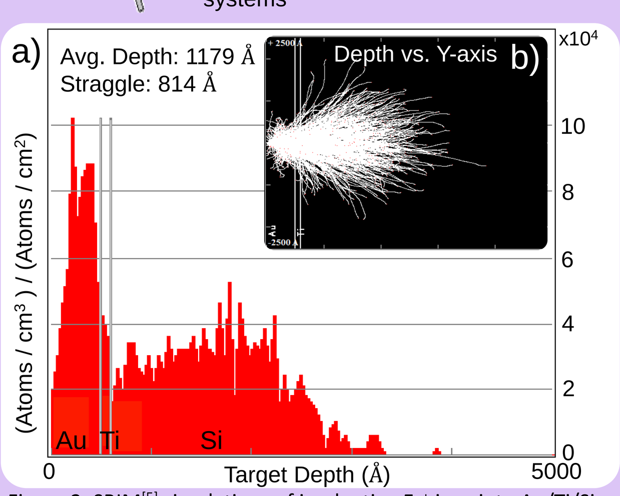

Figure 2: SRIM[5] simulations of implanting Er^+ ions into Au/Ti/Si showing a) the concentration of Er^+ ions with target depth and b) Monte-Carlo simulated paths the implanted ions take in the y-z plane.

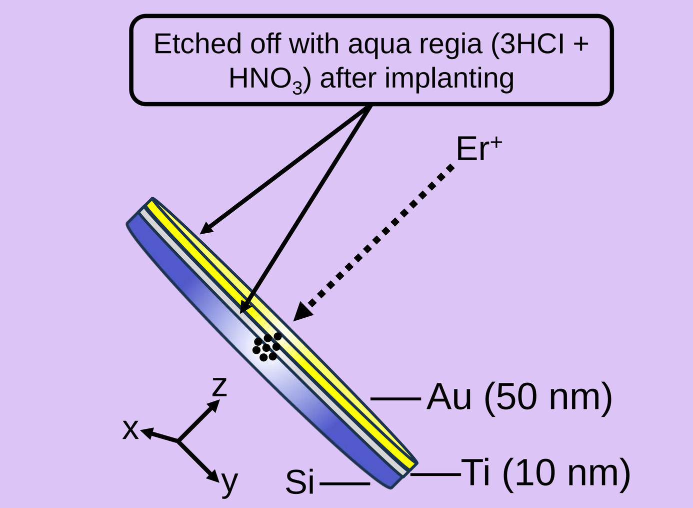

Figure 3: An exaggerated model of the Er^+ into Si implantation layer structure. Au and an adhesive Ti layer were used as a temporary mask to intentionally stop the ions nearer to the surface of the Si substrate.

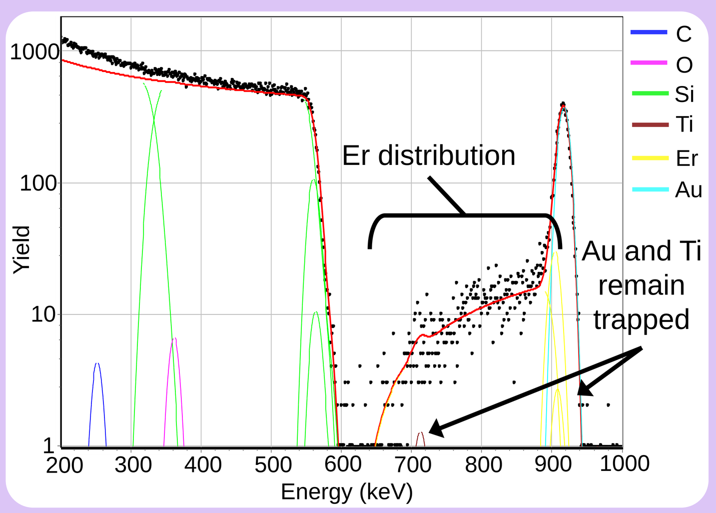

Figure 4: Curve-fit RBS spectrum of the Si wafer after Er^+ implantation and aqua regia etching to remove the Au/Ti masking layer.

Results – XPS

$$B.E. = h\nu - (K.E. + \phi)$$

XPS is used to elucidate the chemical states of REE's within each ore or material. To accurately identify these chemical states, reference spectra of pure REE compounds are needed. These compounds exhibit complex structures and suffer from various broad overlapping Auger peaks in regions of interest, thus higher energy X-rays (Ag Lα) are also being utilized.

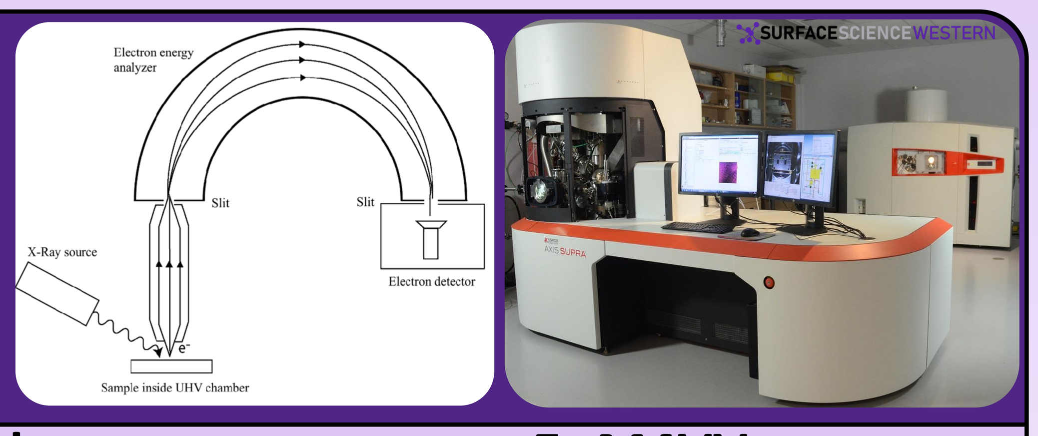

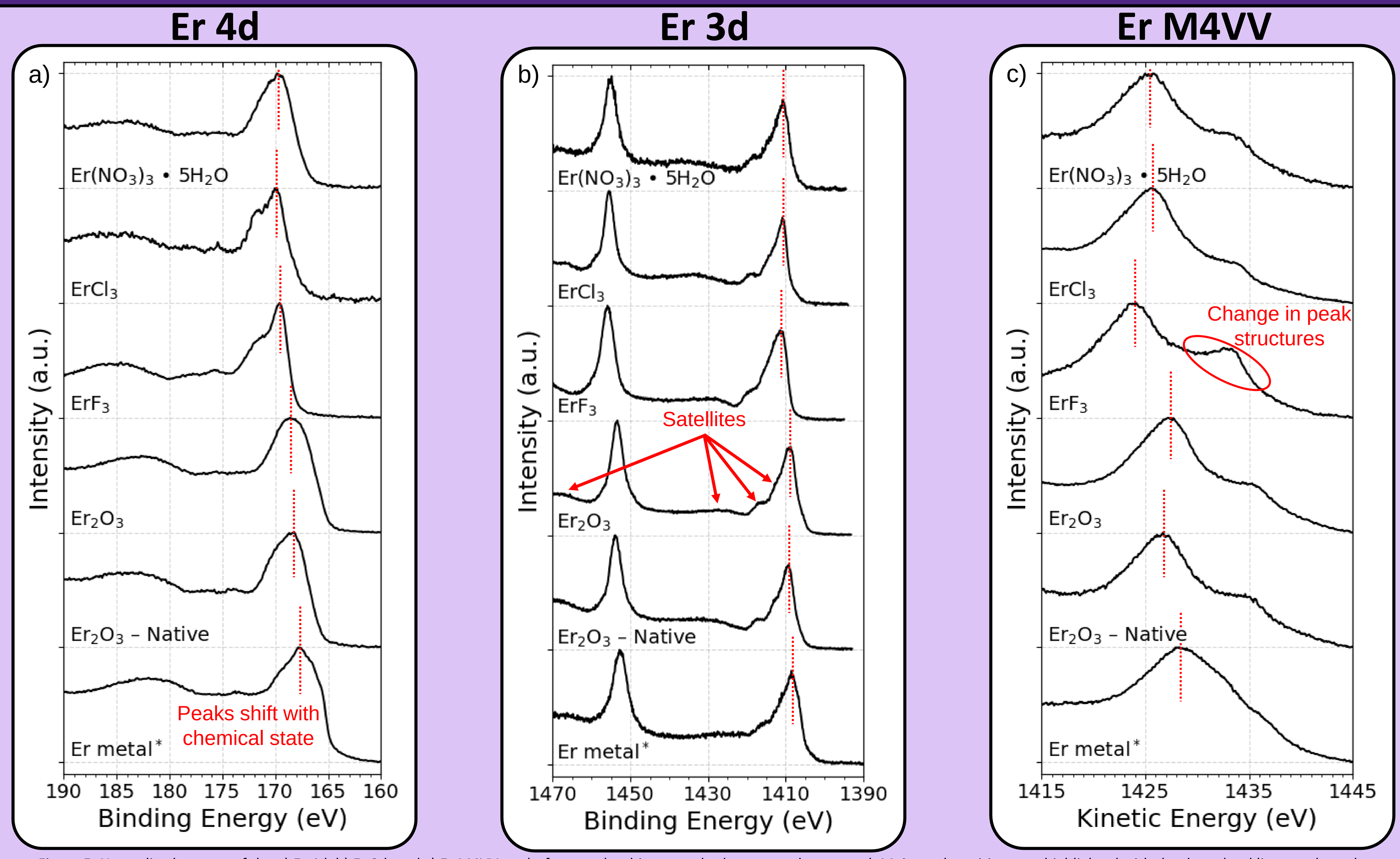

Figure 5: Normalized spectra of the a) Er 4d, b) Er 3d, and c) Er M4VV peaks from each erbium standard compound measured. Main peak positions are highlighted with the dotted red lines to show the shifts observed with changes in chemical state. ***Surface oxide is still observed in Er metal, noted by the presence of the O 1s peak (Figure 6) and rounded Er 4d structure.**[6]

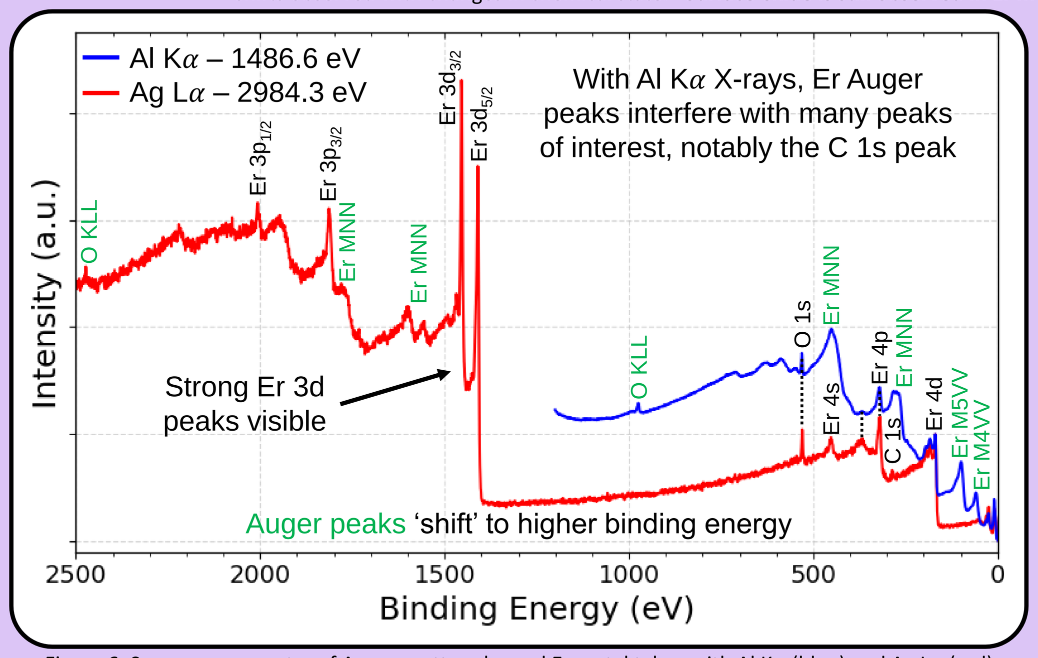

Figure 6: Survey scan spectra of Ar_{500}^+ sputter-cleaned Er metal taken with Al Kα (blue) and Ag Lα (red) X-ray sources. Spectra are normalized to the Er 4d peak at 168 eV. Auger peaks are marked in green.

- Different chemical states exhibit energy shifts and structural changes in all main peaks
- Complex structure and satellites are observed in Er 4d and Er 3d peaks
- Higher energy X-ray's shift Auger peaks and give rise to stronger photoelectron peaks
- Curve-fitting of peak envelopes with constraints should be employed for more accurate speciation
- Elemental ratios from survey quantification and counterion peaks must also be considered and compared to the expected chemistry and stoichiometry
- All high-resolution spectra are charge corrected to the alkyl-type component of C 1s at 284.8 eV

Bastnaesite, (Ce, La, Y)CO_3F

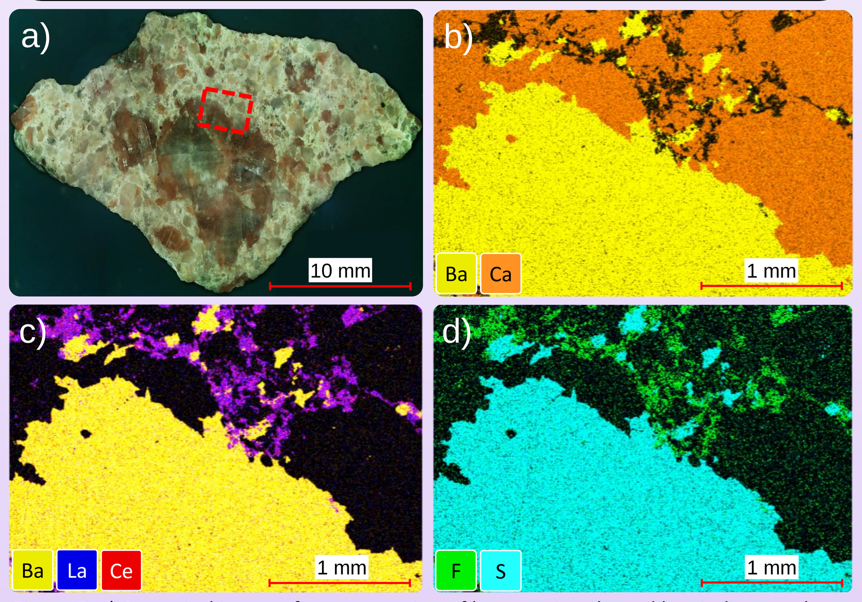

Figure 7: a) An optical image of a cross-section of bastnaesite, the red box indicates where Energy Dispersive X-ray maps were taken of b) barium (yellow) and calcium (orange), c) barium (yellow), lanthanum (blue), and cerium (red), and d) fluorine (green) and sulfur (cyan).

Area	C	O	Ce	La	F	Ca	Ba	S	Sr
Red/Black	11.8	55.3	–	–	–	–	22.0	9.8	1.1
White	9.1	57.0	–	–	–	–	23.2	9.6	0.9
Beige	34.9	35.4	1.0	1.0	1.3	26.4	0.1	–	–

→ $BaSO_4$
→ $CaCO_3$ + (Ce, La)CO_3F

Table 1: XPS survey scan atomic percentages from different areas on the bastnaesite surface. Rare earths detected are highlighted in yellow.

Conclusions and References

- Improvements on methods of detecting, identifying, and quantifying REE's such as XPS can inform and enhance recovery procedures to strengthen REE supply chains from both mining and recycling
- Ion implantation with RBS verification could be a promising method to develop custom calibration standards for SIMS analyses in a semi-affordable and efficient fashion – more testing is needed
- Light REE's were found in interstitial regions between the associated barite ($BaSO_4$) and calcite ($CaCO_3$) mineral grains

[1] Service Canada. "The Canadian Critical Minerals Strategy." (2022)
[2] U.S. Department of the Interior "Mineral Commodity Summaries" (2023)
[3] S.L. Liu et al. *Ore Geology Reviews* 157 (2023):
[4] T. McNulty et al. *MRS Bulletin* 47, no. 3, 258–266 (2022)
[5] J.F. Ziegler et al. *Nuclear Instruments and Methods in Physics Research Section B: Beam Interactions with Materials and Atoms* 268, no. 11, 1818–1823 (2010)
[6] J.F. Moulder et al. *Handbook of X-ray Photoelectron Spectroscopy (1992)*

Acknowledgements

This work is supported by Natural Science and Engineering Research Council of Canada (NSERC) Discovery Grants as well as funding from the Canadian Foundation for Innovation and Ontario Research Fund for the Kratos AXIS Supra spectrometer. The mineral samples analyzed in this work were supplied by the Dana Collection, courtesy of the Richard W. Hutchison Geoscience Collaborative Suite. Special thanks to Jack Hendriks for assistance in operating the Tandetron Accelerator, Dr. Todd Simpson and Tim Goldhawk from the Western nanofabrication facility for the implant mask depositions and initial mask removal, and Dr. Jeffrey Henderson for assistance in XPS and EDX analyses and processing.